CFTR Functions as a Bicarbonate Channel in Pancreatic Duct Cells

Hiroshi Ishiguro,[1] Martin C. Steward,[3] Satoru Naruse,[2] Shigeru B.H. Ko,[2] Hidemi Goto,[2] R. Maynard Case,[3] Takaharu Kondo,[1] and Akiko Yamamoto[1]

[1]Human Nutrition and [2]Gastroenterology, Nagoya University Graduate School of Medicine, Nagoya 466-8550, Japan
[3]Faculty of Life Sciences, University of Manchester, Manchester M13 9NT, England, UK

Pancreatic duct epithelium secretes a HCO_3^--rich fluid by a mechanism dependent on cystic fibrosis transmembrane conductance regulator (CFTR) in the apical membrane. However, the exact role of CFTR remains unclear. One possibility is that the HCO_3^- permeability of CFTR provides a pathway for apical HCO_3^- efflux during maximal secretion. We have therefore attempted to measure electrodiffusive fluxes of HCO_3^- induced by changes in membrane potential across the apical membrane of interlobular ducts isolated from the guinea pig pancreas. This was done by recording the changes in intracellular pH (pH_i) that occurred in luminally perfused ducts when membrane potential was altered by manipulation of bath K^+ concentration. Apical HCO_3^- fluxes activated by cyclic AMP were independent of Cl^- and luminal Na^+, and substantially inhibited by the CFTR blocker, $CFTR_{inh}$-172. Furthermore, comparable HCO_3^- fluxes observed in ducts isolated from wild-type mice were absent in ducts from cystic fibrosis (ΔF) mice. To estimate the HCO_3^- permeability of the apical membrane under physiological conditions, guinea pig ducts were luminally perfused with a solution containing 125 mM HCO_3^- and 24 mM Cl^- in the presence of 5% CO_2. From the changes in pH_i, membrane potential, and buffering capacity, the flux and electrochemical gradient of HCO_3^- across the apical membrane were determined and used to calculate the HCO_3^- permeability. Our estimate of ∼0.1 μm sec^{-1} for the apical HCO_3^- permeability of guinea pig duct cells under these conditions is close to the value required to account for observed rates of HCO_3^- secretion. This suggests that CFTR functions as a HCO_3^- channel in pancreatic duct cells, and that it provides a significant pathway for HCO_3^- transport across the apical membrane.

The Journal of General Physiology

INTRODUCTION

Pancreatic duct epithelium secretes a HCO_3^--rich isotonic fluid that acts as a vehicle for the protein-rich secretion from the acinar cells and serves to raise the pH of the duodenal contents. The ductal system of the human pancreas produces ∼2.5 liters of juice per day, the HCO_3^- concentration of which reaches 140 mM at maximal stimulation (Argent et al., 2006). The CFTR, which is located in the apical membrane of the pancreatic duct cells (Crawford et al., 1991; Marino et al., 1991), is thought to play a key role in ductal HCO_3^- secretion. Severe loss of CFTR function due to mutation causes impaired ductal HCO_3^- secretion in cystic fibrosis (Ahmed et al., 2003). Mild dysfunction due to less severe mutations and/or polymorphisms may be responsible for certain cases of idiopathic chronic pancreatitis (Fujiki et al., 2004; Cohn, 2005).

The molecular mechanisms responsible for HCO_3^- uptake across the basolateral membrane of pancreatic duct cells are now well understood. HCO_3^- uptake is mediated both by Na^+–$2HCO_3^-$ cotransport (pNBCe1) and, indirectly, by Na^+–H^+ exchange (NHE1) and H^+-ATPase activity, although the relative contributions of these pathways may vary between species (Steward et al., 2005). In the guinea pig, pNBCe1 accounts for ∼75% of basolateral HCO_3^- uptake (Ishiguro et al., 1996, 1998). Furthermore, the hyperpolarizing effect of this transporter is important in sustaining the membrane potential required to drive HCO_3^- efflux across the apical membrane.

The mechanism by which HCO_3^- crosses the apical membrane is not so clearly defined. The key transporters are CFTR and a Cl^-/HCO_3^- exchanger that is now thought to be a member of the SLC26 family, most probably SLC26A6 (Lohi et al., 2000). The classical view is that CFTR mainly secretes Cl^-, having a relatively low permeability to HCO_3^-, and HCO_3^- subsequently enters the duct lumen by exchange with Cl^-. There is little doubt that this is the predominant mechanism in species such as the rat and mouse, where the pancreatic duct secretes relatively low concentrations of HCO_3^-. However, isolated interlobular ducts from the guinea pig pancreas, like the human pancreas, can secrete HCO_3^- at maximal rates, even when the luminal fluid contains 140 mM HCO_3^-. This would be impossible to achieve by 1:1 exchange of

Correspondence to Hiroshi Ishiguro: ishiguro@htc.nagoya-u.ac.jp

Abbreviations used in this paper: BCECF, 2′7′-bis(2-carboxyethyl)-5(6)-carboxyfluorescein; dbcAMP, dibutyryl cAMP; H_2DIDS, dihydro-4,4′-diisothiocyanatostilbene-2,2′-disulphonic acid; NHE1, Na^+–H^+ exchange; pH_i, intracellular pH; pNBCe1, Na^+–$2HCO_3^-$ cotransport.

The Rockefeller University Press $30.00
J. Gen. Physiol. Vol. 133 No. 3 315–326
www.jgp.org/cgi/doi/10.1085/jgp.200810122

HCO_3^- for Cl^- because the ionic gradients would favor HCO_3^- reabsorption rather than secretion (Sohma et al., 2000; Steward et al., 2005). Even if the stoichiometry of SLC26A6 was $2HCO_3^-$:$1Cl^-$, as has been suggested (Ko et al., 2002; Shcheynikov et al., 2006), the exchanger would be operating very close to equilibrium (Steward et al., 2005; Ishiguro et al., 2007b). Given that CFTR appears to develop an increased HCO_3^- permeability under conditions of low extracellular Cl^- (Shcheynikov et al., 2004), it has been suggested that CFTR might become the main pathway for HCO_3^- efflux across the apical membrane during maximal secretion (Steward et al., 2005; Ishiguro et al., 2007b).

Our previous work has shown that the electrochemical driving force for HCO_3^- secretion across the apical membrane remains strong during maximal secretion mainly because of the tight regulation of intracellular pH (pH_i) and the hyperpolarizing effect of the basolateral pNBCe1 activity (Ishiguro et al., 2000, 2002b). So it is quite possible that HCO_3^- is secreted largely via a conductive pathway rather than by exchange. Furthermore, the driving force for Cl^-, at least in the guinea pig, dwindles to very little because of the cells' limited capacity for basolateral Cl^- uptake (Ishiguro et al., 2002a; Fernandez-Salazar et al., 2004). It is therefore feasible that CFTR secretes more HCO_3^- than Cl^- under these conditions, even if it remains preferentially permeable to Cl^-.

Although the electrochemical gradient favors HCO_3^- secretion via a conductive pathway, the plausibility of this model also depends upon the HCO_3^- permeability of the apical membrane being sufficiently large. Measurement of the latter was therefore the principal aim of this study. Interlobular ducts were isolated from the guinea pig pancreas, stimulated with dibutyryl cAMP (dbcAMP), and luminally perfused with 125 mM HCO_3^- and 24 mM Cl^- to replicate the conditions that exist during maximal secretion. Taking advantage of the basolateral localization of K^+ channels (Novak and Greger, 1988) and the low paracellular resistance of the ductal epithelium (Novak and Greger, 1991), we have used changes in bath K^+ concentration to induce changes in the membrane potential at the apical membrane. From the resulting changes in pH_i we have been able (1) to demonstrate electrodiffusive fluxes of HCO_3^- across the apical membrane, (2) to estimate the HCO_3^- permeability of the apical membrane, and (3) to evaluate the direct contribution of CFTR to HCO_3^- secretion. We conclude that a substantial fraction of the secreted HCO_3^- crosses the apical membrane through CFTR channels rather than by exchange with luminal Cl^-.

MATERIALS AND METHODS

This study was approved by the Ethical Committee on Animal Use for Experiment and the Recombinant DNA Experiment Safety Committee of Nagoya University.

Animals

Female Hartley guinea pigs (350–450 g) were purchased from Japan SLC. A cystic fibrosis mouse model in which the ΔF508 mutation was introduced into the CFTR gene (ΔF mouse; Zeiher et al., 1995) was purchased from The Jackson Laboratory. The mice were maintained on a standard diet, and genotyping was performed on day 14 postpartum as described previously (Zeng et al., 1997).

Isolation of Interlobular Ducts

Animals were killed by cervical dislocation. As described previously (Ishiguro et al., 1996), the pancreas was removed and interlobular ducts (100–150 μm in diameter) were isolated and cultured overnight.

Microperfusion of the Isolated Interlobular Ducts

The lumen of each interlobular duct segment was microperfused (Ishiguro et al., 2000). Both ends of the duct were cut open using sharpened needles, and one end was cannulated with concentric holding and perfusion pipettes (Fig. 1 B). The bath and lumen were perfused separately, and the bath was maintained at 37°C.

Solutions

The standard (normal-K^+) HCO_3^--buffered solution contained (in mM) 35 NaCl, 80 NMDG-Cl, 5 KCl, 1 $CaCl_2$, 1 $MgCl_2$, 10 D-glucose, and 25 $NaHCO_3$, and was equilibrated with 95% O_2 plus 5% CO_2. The standard (normal-K^+) HEPES-buffered solution contained (in mM) 60 NaCl, 80 NMDG-Cl, 5 KCl, 1 $CaCl_2$, 1 $MgCl_2$, 10 D-glucose, and 10 HEPES, and was equilibrated with 100% O_2. High-K^+ (70 mM) solutions were made by replacing NMDG with K^+ so that the Na^+ concentration remained constant at 60 mM. Low-K^+ (1 mM) solutions were made by replacing K^+ with NMDG. The high-HCO_3^- solutions contained 125 mM HCO_3^- and were equilibrated with 95% O_2 plus 5% CO_2, pH ~8.2. The Na^+-free high-HCO_3^- solution was made by replacing Na^+ with NMDG. Cl^--free solutions were made by replacing Cl^- with glucuronate. All solutions, apart from the high-HCO_3^- solution, were adjusted to pH 7.4 at 37°C.

Measurement of pH_i

pH_i in the duct cells was estimated by microfluorometry (Ishiguro et al., 2000) using the pH-sensitive fluoroprobe 2′7′-bis(2-carboxyethyl)-5(6)-carboxyfluorescein (BCECF). After cannulating the duct for luminal perfusion, the duct cells were loaded with BCECF for 10 min by adding 2 μM of the acetoxymethyl ester BCECF-AM to the bathing solution. Small regions of the duct epithelium (10–20 cells; Fig. 1 B) were illuminated alternately at excitation wavelengths of 430 and 480 nm. Values of pH_i were calculated from the fluorescence ratio (F_{480}/F_{430}) measured at 530 nm. The system was calibrated using the high-K^+/nigericin technique.

Measurement of Intracellular Potential

Basolateral membrane potential V_b was measured with respect to the bath by impaling the duct cells with glass microelectrodes (Ishiguro et al., 2002b). Transepithelial potential difference (V_t) was measured by advancing the electrode into the lumen under identical conditions. Apical membrane potential V_a was calculated by subtraction ($V_b - V_t$).

Materials

BCECF-AM and dihydro-4,4′-diisothiocyanatostilbene-2,2′-disulphonic acid (H_2DIDS) were obtained from Invitrogen. dbcAMP was from Sigma-Aldrich. $CFTR_{inh}$-172 was from EMD.

Statistics

Data are presented as the means ± SEM. Tests for statistically significant differences were made with Student's *t* test or the Mann-Whitney *U* test as appropriate.

RESULTS

Electrodiffusive HCO_3^- Fluxes across the Apical Membrane of Guinea Pig Ducts

Initial experiments established whether electrodiffusive transport of HCO_3^- could be detected across the apical membrane of guinea pig interlobular duct cells. The approach was to alter the membrane potential of the cells and record the changes in pH_i that resulted from HCO_3^- movements into or out of the cells across the apical membrane. Because the ductal epithelium is categorized as "leaky" (i.e., the paracellular pathway has a low electrical resistance), it was assumed that changes in basolateral membrane potential, induced by varying the bath K^+ concentration ($[K^+]_B$), would be replicated at the apical membrane and that the absolute values would differ by no more than a few millivolts (Novak and Greger, 1991).

The conditions used in these experiments are summarized in Fig. 1 A. To minimize the movements of HCO_3^- across the basolateral membrane, the bath was perfused with a HCO_3^--free, HEPES-buffered solution. This also contained 0.5 mM H_2DIDS to inhibit HCO_3^- efflux via the basolateral Na^+-HCO_3^- cotransporter and Cl^--HCO_3^- exchanger (Ishiguro et al., 2000, 2002a). The concentrations of Na^+ in the bath and luminal solutions were kept constant at 60 mM throughout these experiments, and $[K^+]_B$ was varied (1, 5, or 70 mM) by substitution with the impermeant organic cation NMDG. Only the luminal solution contained HCO_3^-; therefore, any changes that occurred in pH_i should largely reflect HCO_3^- movements across the apical membrane.

Representative traces from these experiments are shown in Fig. 1 (C and D). Initially, both bath and lumen were perfused with the standard (normal-K^+) HEPES-buffered solution. To simulate the high luminal HCO_3^- and low luminal Cl^- concentrations that exist in the ducts under physiological conditions, the luminal solution was switched after 3 min to one containing 125 mM HCO_3^- and 24 mM Cl^- and equilibrated with 5% CO_2. As described previously (Ishiguro et al., 2000), pH_i fell by almost 1 pH unit (Fig. 1 C) due to CO_2 diffusion into the cells, and it showed no sign of recovery, despite the presence of 125 mM HCO_3^- in the lumen. When $[K^+]_B$ was raised from 5 to 70 mM to depolarize the cells, a maneuver that would be expected to favor HCO_3^- entry

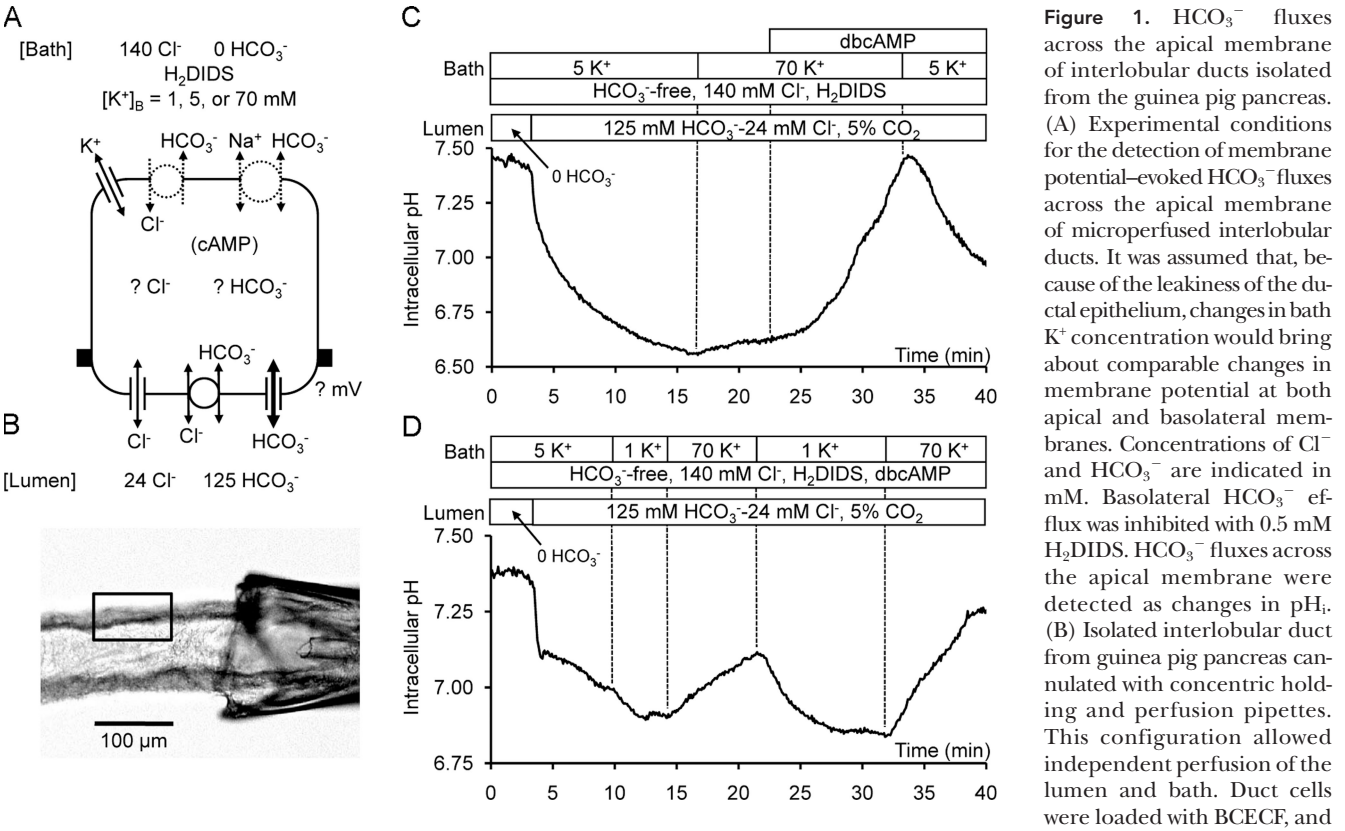

Figure 1. HCO_3^- fluxes across the apical membrane of interlobular ducts isolated from the guinea pig pancreas. (A) Experimental conditions for the detection of membrane potential–evoked HCO_3^- fluxes across the apical membrane of microperfused interlobular ducts. It was assumed that, because of the leakiness of the ductal epithelium, changes in bath K^+ concentration would bring about comparable changes in membrane potential at both apical and basolateral membranes. Concentrations of Cl^- and HCO_3^- are indicated in mM. Basolateral HCO_3^- efflux was inhibited with 0.5 mM H_2DIDS. HCO_3^- fluxes across the apical membrane were detected as changes in pH_i. (B) Isolated interlobular duct from guinea pig pancreas cannulated with concentric holding and perfusion pipettes. This configuration allowed independent perfusion of the lumen and bath. Duct cells were loaded with BCECF, and a small region of the duct epithelium (indicated by the rectangle) was selected for measurement of pH_i. (C and D) Membrane potential–evoked changes in pH_i in ducts exposed to different bath K^+ concentrations. Bath and lumen were first perfused with the standard HEPES-buffered solution, and the luminal solution was then switched to the high-HCO_3^- solution containing 125 mM HCO_3^- and 24 mM Cl^-. 0.5 mM dbcAMP was present in the bath perfusate as indicated. The Na^+ concentration in the bath and luminal solutions was 60 mM throughout, and $[K^+]_B$ was raised or lowered (1, 5, and 70 mM) by replacement with NMDG. Each trace is representative of four experiments.

from the lumen, pH_i increased only slightly (0.10 ± 0.02; $n = 4$) in these unstimulated ducts. However, when the membrane permeant cAMP analogue dbcAMP (0.5 mM) was added to the bath perfusate to stimulate secretion, the increase in pH_i accelerated dramatically (Fig. 1 C). When $[K^+]_B$ was subsequently restored to 5 mM, pH_i also fell rapidly.

In experiments of the type shown in Fig. 1 D, the ducts were stimulated continuously with dbcAMP. When $[K^+]_B$ was switched from 5 to 1 mM to hyperpolarize the cells, pH_i quickly decreased from 6.83 ± 0.11 ($n = 4$) to 6.72 ± 0.09 ($P < 0.05$; paired Student's t test). It then increased steadily when $[K^+]_B$ was raised to 70 mM, reaching 7.32 ± 0.09 ($P < 0.01$) after 7 min. Thus, depolarization and hyperpolarization caused increases and decreases in pH_i, respectively. These changes are consistent with HCO_3^- moving across the apical membrane according to its electrochemical gradient via a HCO_3^- conductance activated by intracellular cAMP.

Cl^- and Na^+ Dependence of Apical HCO_3^- Fluxes in Guinea Pig Ducts

Electrodiffusion through an anion channel such as CFTR provides one possible explanation for these results. However, alternative pathways might account for membrane potential–induced HCO_3^- movements across the apical membrane. These include electrogenic Na^+-$nHCO_3^-$ cotransporters and electrogenic SLC26 transporters that mediate Cl^--$nHCO_3^-$ exchange, such as SLC26A6 (Ko et al., 2002; Shcheynikov et al., 2006). To evaluate their contribution, we next examined whether the apical fluxes of HCO_3^- induced by membrane potential changes were dependent on the presence of Cl^- (Fig. 2 A) or luminal Na^+ (Fig. 2 B).

In the Cl^--free experiments, such as the one shown in Fig. 2 A, the bath and lumen of ducts stimulated with dbcAMP were initially perfused for 30 min with Cl^--free, HEPES-buffered solution (normal-K^+). The expectation was that Cl^- would leave the cells via activated CFTR channels, and that the intracellular Cl^- concentration ($[Cl^-]_i$) would be close to zero by the time the experiment was begun. As before, switching the luminal solution to the high-HCO_3^-, Cl^--free solution (0 mM Cl^-, 125 mM HCO_3^-, 5% CO_2) caused pH_i to fall rapidly as a result of CO_2 entry into the cells (Fig. 2 A). When $[K^+]_B$ was reduced from 5 to 1 mM and then raised to 70 mM, with dbcAMP present throughout, pH_i decreased from 7.15 ± 0.06 ($n = 4$) to 7.06 ± 0.07 and then increased steadily, reaching 7.54 ± 0.16 after 8 min. These results are very similar to those observed in the presence of Cl^- (Fig. 1 D), which suggests that electrogenic Cl^--$nHCO_3^-$ exchange does not contribute significantly to the observed fluxes of HCO_3^- across the apical membrane under these conditions.

To examine the Na^+ dependence of the apical HCO_3^- fluxes, all of the Na^+ in the luminal solution was replaced with NMDG, while the bath Na^+ concentration remained at 60 mM. In all other respects the protocol was the same as in Figs. 1 D and 2 A, with 125 mM HCO_3^- in the lumen and continuous stimulation applied with dbcAMP. When $[K^+]_B$ was raised from 1 to 70 mM, pH_i rose steadily as before, increasing from 6.96 ± 0.08 ($n = 4$) to 7.36 ± 0.11 after 8 min. Because the rate of increase in pH_i was unaffected by the presence or absence of luminal Na^+, we conclude that electrogenic Na^+-$nHCO_3^-$ cotransport does not contribute significantly to the depolarization-evoked influx of HCO_3^- across the apical membrane.

Collectively, these data suggest that the movements of HCO_3^- that result from manipulation of the membrane

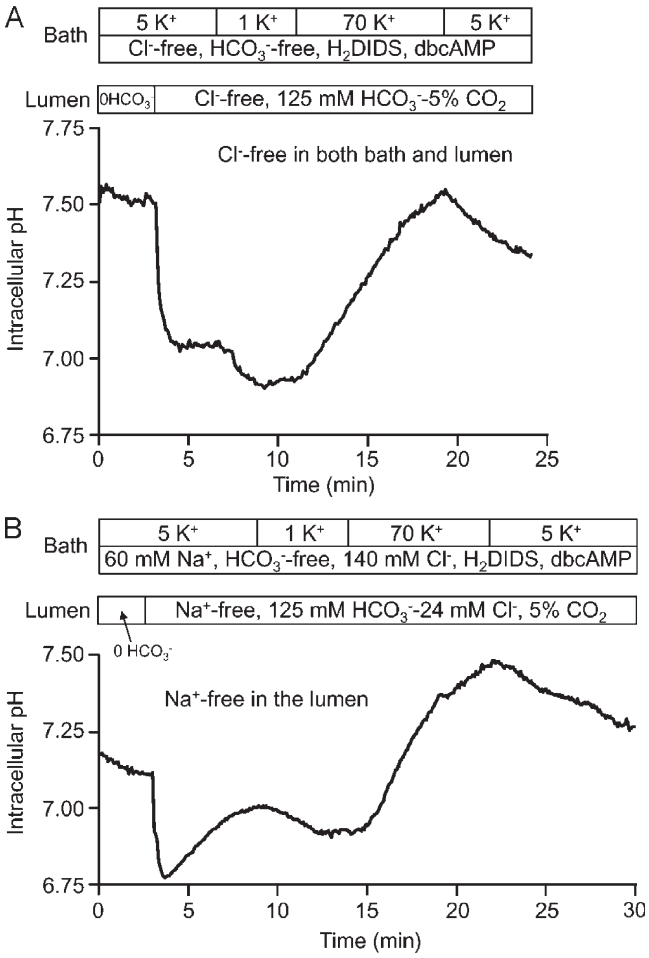

Figure 2. Cl^- and Na^+ dependence of HCO_3^- fluxes across the apical membrane of guinea pig pancreatic ducts. (A) Membrane potential–evoked changes in pH_i in the absence of Cl^-. To deplete intracellular Cl^-, the bath and lumen were perfused with the Cl^--free, HEPES-buffered solution in the presence of dbcAMP for 30 min before the measurements. Experimental conditions were similar to those in Fig. 1 D, but with Cl^- replaced by glucuronate in both the bath and luminal perfusates. Representative of four experiments. (B) Membrane potential–evoked changes in pH_i in the absence of luminal Na^+. Experiments were similar to those shown in Fig. 1, but with Na^+ replaced by NMDG in the luminal perfusate. Representative of four experiments.

potential are mediated by a cAMP-activated HCO_3^- conductance in the apical membrane.

Effect of $CFTR_{inh}$-172 on Apical HCO_3^- Fluxes in Guinea Pig Ducts

To explore the possibility that the apical HCO_3^- conductance in stimulated guinea pig ducts is due to the presence of CFTR, we next tested the effect of adding the selective blocker $CFTR_{inh}$-172 to the luminal perfusate (Fig. 3). The experimental conditions and protocol were otherwise similar to those used in the experiments shown in Fig. 1. 2 min after applying 5 μM $CFTR_{inh}$-172 to the apical membrane, the rise in pH_i evoked by switching $[K^+]_B$ from 1 to 70 mM (Fig. 3 A) was significantly slower than in the absence of the blocker. The rate of increase in pH_i was reduced from 0.158 ± 0.030 pH units min^{-1} ($n = 6$) to 0.066 ± 0.023 pH units min^{-1} ($n = 6$; $P < 0.05$), representing a mean inhibition of 61 ± 7% in the presence of $CFTR_{inh}$-172.

Furthermore, when $CFTR_{inh}$-172 was removed from the luminal perfusate during basolateral exposure to 70 mM K^+ (Fig. 3 B), the increase in pH_i accelerated as the block was reversed. These results support the idea that much of the apical membrane HCO_3^- conductance is carried by CFTR.

Apical HCO_3^- Fluxes in Ducts Isolated from Normal and Cystic Fibrosis Mice

As a further test of this hypothesis, we performed a small number of similar experiments on interlobular ducts isolated from a cystic fibrosis mouse model (ΔF) in which the ΔF508 mutation has been introduced into the CFTR gene. Experiments were performed in the absence of Cl^- to eliminate any possible contribution from apical anion exchangers, and the protocol was similar to that used in Fig. 2 A. The bath was perfused with a Cl^-- and HCO_3^--free, HEPES-buffered solution containing H_2DIDS and dbcAMP, and the lumen was perfused with a high-HCO_3^-, Cl^--free solution (0 mM Cl^-, 125 mM HCO_3^-, 5% CO_2).

In ducts isolated from wild-type mice, membrane hyperpolarization and depolarization evoked by lowering and raising $[K^+]_B$ caused decreases and increases in pH_i (Fig. 4 A), which were similar to those observed in the guinea pig ducts. In ducts isolated from the ΔF mice (Fig. 4 B), however, these changes in pH_i were almost entirely abolished. This result strongly supports the conclusion that, in mice at least, the electrodiffusive fluxes of HCO_3^- that we have observed across the apical membrane are carried largely by CFTR.

Estimation of the Apical HCO_3^- Permeability of Guinea Pig Ducts

Our next task was to determine whether the apical HCO_3^- permeability would be sufficient to account for the rates of HCO_3^- secretion that are observed in isolated guinea pig ducts. For these experiments, the bath perfusate contained 25 mM HCO_3^- so that, like the luminal perfusate, it could be equilibrated with 5% CO_2. It was important that the luminal and bath pCO_2 values, and therefore the intracellular pCO_2, were the same because a value for the latter is required (1) to calculate $[HCO_3^-]_i$ from pH_i and (2) to determine the intracellular buffering capacity. Including 25 mM HCO_3^- in the bath perfusate required the additional, but justifiable, assumption that HCO_3^- entry across the basolateral membrane would be adequately blocked by the H_2DIDS in the bath perfusate.

As before, the lumen was perfused with the high-HCO_3^- solution (24 mM Cl^-, 125 mM HCO_3^-, 5% CO_2),

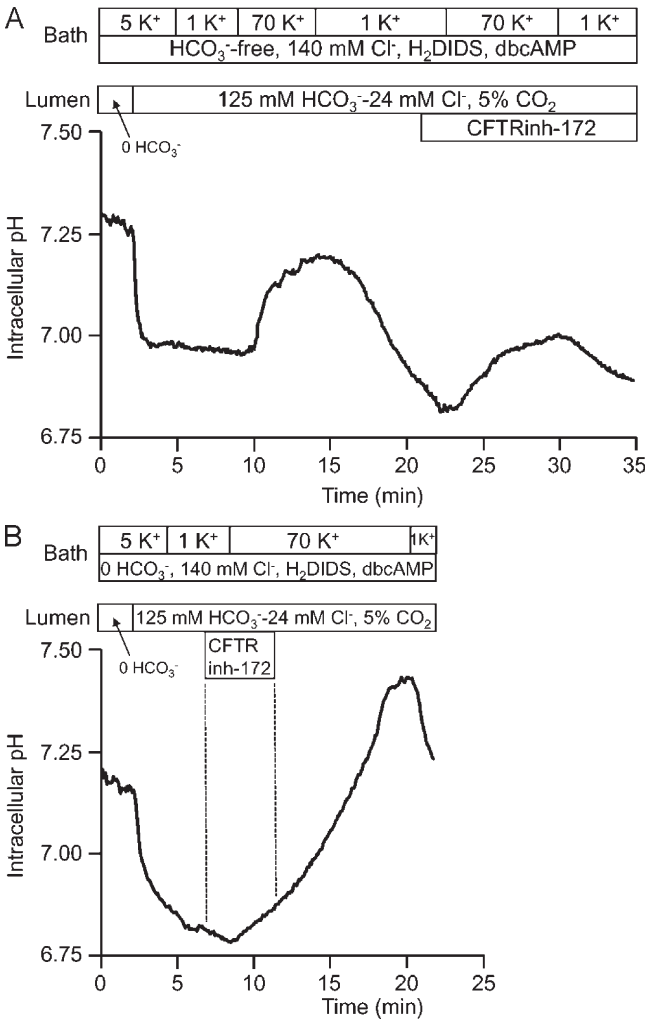

Figure 3. Inhibition of HCO_3^- fluxes across the apical membrane of guinea pig pancreatic ducts by $CFTR_{inh}$-172. Membrane potential–evoked changes in pH_i in the presence or absence of 5 μM of luminal $CFTR_{inh}$-172 as indicated. Experimental conditions were similar to those in Fig. 1 D. (A) Reduced rate of increase in pH_i evoked by depolarization with 70 mM K^+ when $CFTR_{inh}$-172 was added to the luminal perfusate. (B) Recovery of pH_i increase evoked by 70 mM K^+ when $CFTR_{inh}$-172 was removed from the luminal perfusate. Representative of six experiments.

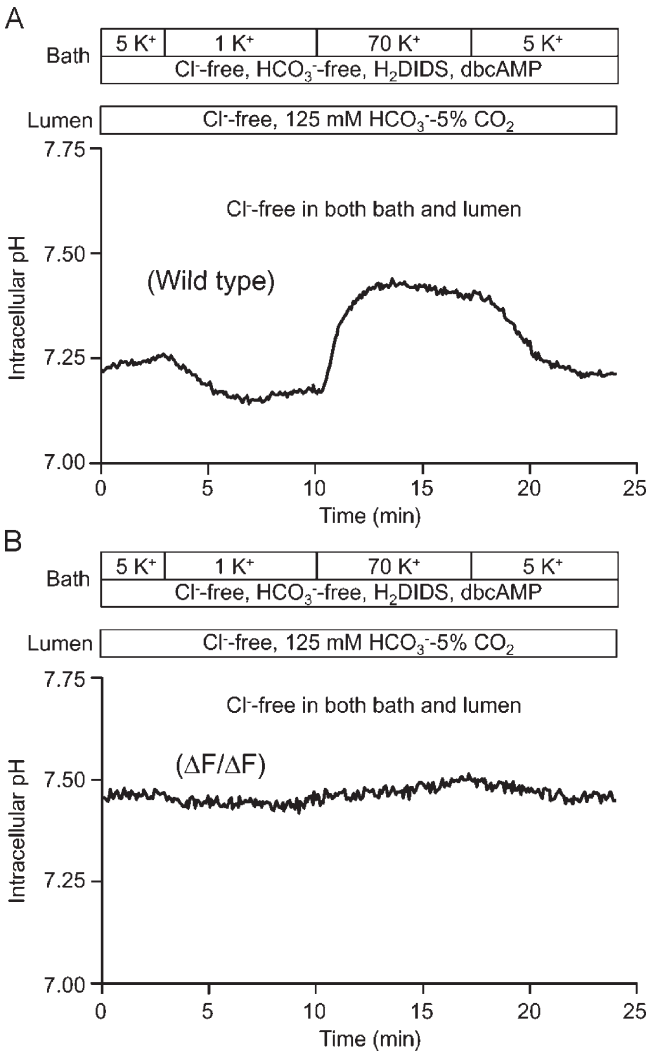

Figure 4. HCO_3^- fluxes across the apical membrane of interlobular pancreatic ducts isolated from wild-type and ΔF mice. Membrane potential–evoked changes in pH_i in interlobular pancreatic ducts isolated from wild-type (A) and ΔF/ΔF (B) mice. Experiments were performed in the bilateral absence of Cl^- following a similar protocol to that used in the guinea pig duct experiment shown in Fig. 2 A. Each trace is a representative of four experiments.

and the cells were depolarized or hyperpolarized by manipulation of $[K^+]_B$ (Fig. 5 A). Fig. 5 B shows a representative trace of the basolateral membrane potential V_b measured with a conventional microelectrode during one of these experiments. The addition of H_2DIDS to the bath perfusate caused a significant depolarization, most probably due to the inhibition of HCO_3^- uptake via the basolateral Na^+-HCO_3^- cotransporter. Thereafter, V_b changed rapidly and reproducibly as $[K^+]_B$ was stepped through a sequence of changes between 70, 5, and 1 mM (Fig. 5 B). The mean values of V_b measured at these three K^+ concentrations were −38.5 ± 2.7 (n = 8), −49.4 ± 1.7 (n = 11), and −58.7 ± 2.7 mV (n = 6), respectively.

Pancreatic duct epithelium is believed to be a low-resistance epithelium (Novak and Greger, 1991), so the apical membrane potential V_a, the critical value required for the calculation of apical HCO_3^- permeability, would be expected to lie close to V_b. However, measurements of the transepithelial potential difference V_t, under the conditions of these experiments, revealed that there was a small difference and that it varied with $[K^+]_B$ (Fig. 5 C). Mean values of V_t (lumen relative to bath) were −1.7 ± 0.1 (n = 8), −3.5 ± 0.1 (n = 12), and −4.1 ± 0.2 mV (n = 6) in 70, 5, and 1 mM K^+. These, together with the corresponding mean values for V_b, were used to calculate best estimates of V_a, which were −37, −46, and −55 mV, respectively.

Changes in pH_i were measured under exactly the same experimental conditions. As V_a became depolarized or hyperpolarized as a result of the step changes in $[K^+]_B$, pH_i increased or decreased accordingly (Fig. 5 D). The steady-state pH_i values that were approached when $[K^+]_B$ was stepped between 70, 5, and 1 mM were 7.34 ± 0.05 (n = 8), 7.18 ± 0.02 (n = 5), and 7.07 ± 0.03 (n = 7), respectively. These lie reasonably close to the values that would be predicted (7.45, 7.30, and 7.15) if HCO_3^- was distributed at electrochemical equilibrium with measured membrane potential values.

The rate of change of pH_i (dpH_i/dt) during these transitions was calculated by linear regression at 1-min intervals (Fig. 6 A). At each time point, the HCO_3^- flux across the apical membrane, J_{HCO3}, was calculated from dpH_i/dt using the following expression:

$$J_{HCO_3} = \frac{dpH_i}{dt} \cdot \beta_t \cdot h, \quad (1)$$

where β_t is the total intracellular buffering capacity (values from Szalmay et al., 2001), and h is the volume of the epithelium per unit area. Assuming that the volume of the lateral intercellular spaces is negligible, the epithelial volume per unit area is equivalent to the cell height, which was estimated to be 10 μm (Argent et al., 1986; Arkle et al., 1986).

The apical HCO_3^- permeability P_{HCO3} was then calculated from each value of J_{HCO3} on the assumption that the apical HCO_3^- flux obeys the Goldman-Hodgkin-Katz equation:

$$J_{HCO_3} = -P_{HCO_3} \frac{zFV_a}{RT} \left(\frac{[HCO_3^-]_L - [HCO_3^-]_i \exp\left(\frac{zFV_a}{RT}\right)}{1 - \exp\left(\frac{zFV_a}{RT}\right)} \right),$$

where z, F, R, and T have their usual meaning. The intracellular HCO_3^- concentration ($[HCO_3^-]_i$) was calculated from pH_i, assuming that the intracellular pCO_2 was 38 mmHg, the intracellular CO_2 solubility was 0.0316 mM $mmHg^{-1}$, and the effective pK_a for HCO_3^-/CO_2 was 6.03 (Edsall and Wyman, 1958). The luminal HCO_3^-

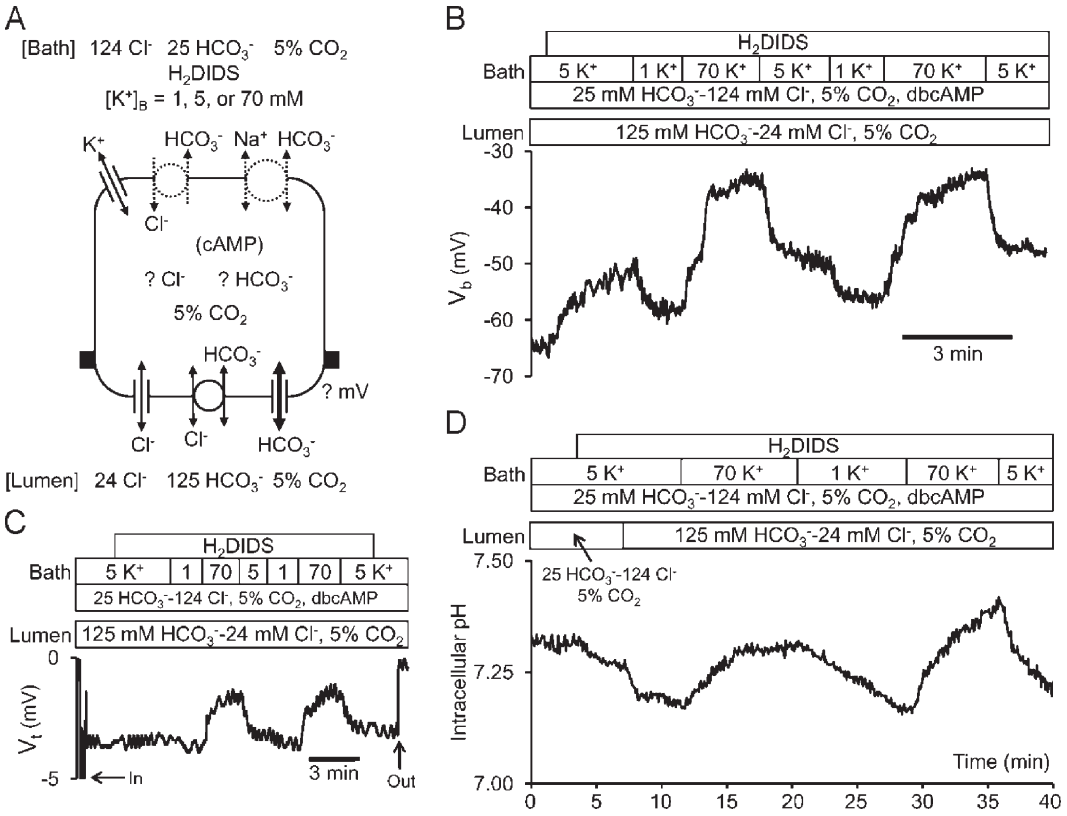

Figure 5. Changes in membrane potential and HCO_3^- fluxes across the apical membrane of guinea pig pancreatic ducts. (A) Experimental conditions used for the measurement of apical HCO_3^- permeability in microperfused interlobular ducts. In this case, the bath perfusate contained 25 mM HCO_3^- and was equilibrated with 5% CO_2. This ensured that pCO_2 was constant throughout the system. All other conditions were the same as in Fig. 1 A. (B) Changes in basolateral membrane potential V_b recorded with a conventional microelectrode when the bath K^+ concentration was switched between 1, 5, and 70 mM. Representative of five experiments. (C) Changes in transepithelial potential difference V_t with the tip of the electrode advanced into the duct lumen. Representative of four experiments. (D) Membrane potential–evoked changes in pH_i recorded under the same conditions as in B. Representative of five experiments.

concentration ($[HCO_3^-]_L$) was 125 mM throughout. The values of V_a used for the calculation were −37, −46, and −55 mV at $[K^+]_B$ values of 70, 5, and 1 mM, respectively.

Calculated values of P_{HCO3} pooled from all of these experiments are shown in Fig. 6 B, where they are separated into two groups according to whether they were estimated from HCO_3^- influx (after depolarization) or HCO_3^- efflux (after hyperpolarization). Both sets of data were widely dispersed, and there was no statistically significant difference between the two mean values: 0.083 ± 0.018 μm sec^{-1} for influx (n = 18 from 5 experiments) and 0.120 ± 0.020 μm sec^{-1} for efflux (n = 18 from 5). The combined mean value for P_{HCO3} was 0.102 ± 0.013 μm sec^{-1} (n = 36 from 5).

An alternative way of analyzing these results is shown in Fig. 6 C. Here, we compare theoretical predictions of the changes in pH_i, assuming three different values for P_{HCO3}, with averaged data from four representative experiments. In this example, $[K^+]_B$ was switched from 1 to 70 mM and then to 1 mM, and the corresponding changes in V_a (Fig. 6 C, top) have been assumed to occur with a time constant of 45 s, as estimated from our microelectrode recordings (e.g., Fig. 5 B). In the bottom of Fig. 6 C, the apical fluxes of HCO_3^- and the consequent changes in pH_i have been calculated in 1-s steps for P_{HCO3} values of 0.05, 0.1, and 0.2 μm sec^{-1}. Comparing the experimental data with the predicted changes, it is clear that the initial rise in pH_i, due to HCO_3^- influx when V_a depolarizes, is consistent with a P_{HCO3} value of ∼0.1 μm sec^{-1}. Thereafter, pH_i increases more slowly than predicted. The initial fall in pH_i, due to HCO_3^- efflux when V_a repolarizes to −55 mV (1 mM K^+), is also fitted well by assuming a P_{HCO3} value of 0.1 μm sec^{-1}, but pH_i appears to approach a slightly lower value than predicted.

DISCUSSION

The aim of this study was to measure voltage-driven fluxes of HCO_3^- through conductive pathways in the apical membrane of guinea pig duct cells. Using these data to estimate the HCO_3^- permeability of the apical membrane, we hoped to find out how much of the HCO_3^- secretion that occurs under physiological conditions is

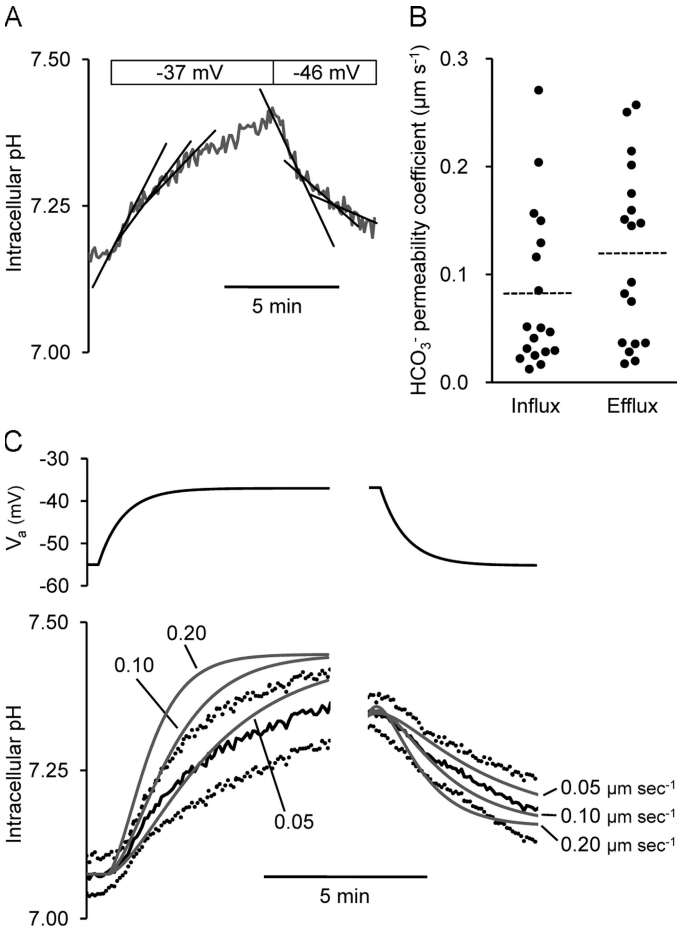

Figure 6. Estimation of apical HCO_3^- permeability. (A) Calculation of the rate of change of pH_i by linear regression at 1-min intervals after step changes in $[K^+]_B$. The fitted lines are overlaid on data from the second half of the experiment shown in Fig. 5 D. Together with the midpoint value of pH_i and the intracellular buffering capacity, these data were used to calculate the HCO_3^- flux across the apical membrane. (B) Distribution of calculated HCO_3^- permeabilities for HCO_3^- influx ($n = 18$ from 5 ducts) and HCO_3^- efflux ($n = 18$ from 5 ducts) pooled from experiments like the one shown in A. The horizontal dotted lines indicate the mean values. (C) Predicted changes in pH_i resulting from changes in V_a induced by switching $[K^+]_B$ from 1 to 70 mM, and then back to 1 mM. Theoretical curves based on three alternative apical HCO_3^- permeability values (0.05, 0.1, and 0.2 µm sec^{-1}) are superimposed on averaged data from four experiments of the type shown in Fig. 5 D. The dotted lines indicate the mean ± SEM. The top panel shows the predicted changes in V_a, assuming a time constant of 45 s.

mediated directly by CFTR rather than by an associated anion exchanger.

To eliminate HCO_3^- movements via other pathways, the HCO_3^- transporters present in the basolateral membrane (pNBCe1 and AE2) were blocked throughout these experiments with H_2DIDS. Membrane potential was altered by manipulation of basolateral K^+ concentration, and care was taken to keep extracellular Na^+ constant at 60 mM. What we believe to be electrodiffusive fluxes of HCO_3^- across the apical membrane were detected as increases and decreases in pH_i after depolarization and hyperpolarization. As $[K^+]_B$ was stepped between 1, 5, and 70 mM, the apical membrane potential of the duct cells moved swiftly between −55, −46, and −37 mV, respectively. The corresponding changes in pH_i were slower, but in each case pH_i moved toward the steady-state value (7.15, 7.30, or 7.45) that would be expected if HCO_3^- redistributed itself passively across the apical membrane according to the new membrane potential. Furthermore, we observed that the changes in pH_i (1) were stimulated by cAMP, (2) were not dependent on the presence of Cl^-, (3) were not dependent on luminal Na^+, (4) were significantly blocked by luminal $CFTR_{inh}$-172, and (5) were absent in ducts isolated from ΔF mice that lacked functional CFTR.

The most plausible explanation for these results is that raising or lowering membrane potential leads to electrodiffusive movements of HCO_3^- across the apical membrane via a conductive pathway, most probably CFTR. Because the high luminal HCO_3^- and low luminal Cl^- concentrations chosen for these experiments closely resemble those that exist during maximal stimulation in vivo, we believe that CFTR, acting as a HCO_3^- channel, makes a significant direct contribution to the secretion of HCO_3^- by the pancreatic duct epithelium.

Estimation of Apical HCO_3^- Permeability

To estimate the direct contribution of CFTR to HCO_3^- secretion, we attempted to measure the HCO_3^- permeability of the apical membrane under conditions as close as possible to physiological. Our previous work had shown that there is a substantial driving force for electrodiffusive HCO_3^- efflux from the cells during maximal stimulation. The aim here was to determine whether the HCO_3^- permeability of the apical CFTR channels was sufficient to make a significant contribution to the total secretory flux of HCO_3^-.

In these experiments, apical HCO_3^- permeability was estimated from the measured HCO_3^- fluxes and the corresponding driving forces when the membrane

potential was stepped between different values. In each experiment, the HCO_3^- flux was estimated at a series of time points from the rate of change of pH_i and the buffering capacity of the cytoplasm. The electrochemical gradient was calculated at each time point from the current pH_i value and the membrane potential, which was measured in a parallel series of experiments.

Most of our individual estimates of P_{HCO3} lie between 0.02 and 0.2 μm s^{-1}, with mean values of around 0.1 μm s^{-1} for both influx and efflux (Fig. 6 B). An alternative, curve-fitting approach also suggests that the value is most likely to be around 0.1 μm s^{-1}. Before drawing any conclusions from these values, it is important to consider some of the possible sources of error and some of the assumptions that have been made in performing the calculations.

1. Other Acid/Base Transporters. In our calculations, we have assumed that the changes in pH_i evoked by alterations in membrane potential were due solely to electrodiffusive HCO_3^- movements across the apical membrane via a conductive pathway. In other words, we believe that the chosen experimental conditions eliminated any significant contributions from other H^+ or HCO_3^- transporters. Certainly the H_2DIDS in the bath solution would have adequately blocked HCO_3^- efflux or influx via the basolateral pNBCe1 and anion exchanger (Ishiguro et al., 2000, 2002a), but the basolateral NHE1 would still have been active in these experiments. This would not have had much effect on pH_i changes at or above normal values, but it would have become increasingly active when pH_i dropped to lower values. Thus, in the case where V_a was hyperpolarized by switching $[K^+]_B$ to 1 mM, the pH_i drop due to HCO_3^- efflux could have been partially offset by increased H^+ extrusion via NHE1. This in turn would have led to underestimation of P_{HCO3}. However, we have noted previously that NHE1 activity is quite low in stimulated guinea pig duct cells (Ishiguro et al., 1996), and the fact that pH_i readily approached the equilibrium value for HCO_3^- (7.15) at −55 mV suggests that the contribution of NHE1 was minimal in these experiments.

The apical Cl^-/HCO_3^- exchanger would have also remained active in these experiments, although the high luminal HCO_3^- and low luminal Cl^- concentrations would have ensured that it was very close to equilibrium. Furthermore, an electrically neutral exchanger would not contribute directly to pH_i changes induced by hyper- or depolarization. But there is now strong evidence to suggest that the apical anion exchanger in pancreatic duct cells is SLC26A6 (Lohi et al., 2000; Ishiguro et al., 2007b), and there are some indications to suggest that it may be electrogenic, mediating a 2:1 exchange of intracellular HCO_3^- for extracellular Cl^- (Ko et al., 2002; Shcheynikov et al., 2006). On the other hand, there may be species differences in stoichiometry, and there are undoubtedly some discrepancies in the literature (Chernova et al., 2005). It is also not clear whether a $2HCO_3^-$:$1Cl^-$ stoichiometry would remain the same when the transporter reverses. Nonetheless, we have to consider the possibility that an electrogenic exchanger responded to the changes in membrane potential that were used in these experiments.

If HCO_3^- and Cl^- were individually at equilibrium in the steady states approached in these experiments, it can be shown that a $2HCO_3^-$:$1Cl^-$ exchanger would also be at equilibrium, as would a 1:1 neutral exchanger. However, suddenly changing V_a would immediately affect the 2:1 exchanger, but not the 1:1 exchanger. Depolarization would favor HCO_3^- influx via a 2:1 exchanger, thus adding to the HCO_3^- influx via CFTR, and hyperpolarization would favor HCO_3^- efflux. Significant fluxes of this kind could have led to overestimation of P_{HCO3} in our experiments.

Our reasons for concluding that the contribution of a 2:1 exchanger is small are (1) the minimal change in voltage-driven HCO_3^- fluxes that we observed in Cl^--free conditions (Fig. 2 A) and (2) the 60% inhibition of HCO_3^- entry observed in the presence of $CFTR_{inh}$-172 (Fig. 3). Given that $CFTR_{inh}$-172 may not achieve a complete block of CFTR after 2 min of exposure at this concentration (Wang et al., 2006; Tang et al., 2008), the figure of 60% must be viewed as a minimum estimate of the fraction of the electrodiffusive HCO_3^- flux that was mediated by CFTR.

2. Cell Volume. To extract HCO_3^- flux data from changes in pH_i, one needs to know both the volume of the cells and the buffering capacity of the cytoplasm. Because our fluxes were calculated per unit area of epithelium, the cell volume per unit area is sufficient, and this is well approximated by the cell height if the lateral intercellular spaces are small. This tends to be the case in secretory epithelia, and the assumption is supported by electron micrographs of interlobular ducts from several species (Egerbacher and Bock, 1997). However, to our knowledge, there are no published values for cell height in any species, and our assumed value of 10 μm is based on visual inspection of published light micrographs of rat ducts (Argent et al., 1986; Arkle et al., 1986) and our own light microscope images of isolated guinea pig ducts. There could therefore be a significant error in this parameter value. If cell height is actually >10 μm, P_{HCO3} will have been underestimated and, if <10 μm, it will have been overestimated.

We are also assuming that this is the correct value for cell volume under the slightly artificial conditions of these experiments. Cell volume in secretory epithelia is tightly linked to intracellular Cl^- content (e.g., Foskett, 1990), so the combination of a high apical Cl^- conductance (due to activated CFTR) and low luminal Cl^- concentration (24 mM) could have resulted in significant

Cl^- loss and cell shrinkage even in the baseline condition for these experiments, particularly with the basolateral transporters disabled. More significantly, the hyperpolarization induced by lowering $[K^+]_B$ could have resulted in a further loss of K^+ and Cl^- from the cell and therefore further cell shrinkage. Conversely, there could have been a net gain of K^+ and Cl^-, and cell swelling when $[K^+]_B$ was raised.

3. Buffering Capacity. Calculation of the apical HCO_3^- fluxes also requires knowledge of the buffering capacity of the cytoplasm and its dependence on pH_i. The values used here were based on a quadratic function fitted to individual estimates of intrinsic buffering capacity that were obtained under slightly different experimental conditions and which showed a significant degree of scatter (Szalmay et al., 2001). The level of uncertainty in β_t could be as large as ±50%, which would have had a comparable effect on our estimates of P_{HCO3}.

The situation is complicated further by the fact that the buffering capacity would have changed as a result of any osmotic swelling or shrinkage of the cells that occurred when $[K^+]_B$ was altered. For example, cell shrinkage would cause the concentration of macromolecular buffering sites and impermeant buffers to increase, thereby raising the intrinsic component of β_t. P_{HCO3} might therefore be underestimated; however, the increase in buffering capacity would be offset by the corresponding decrease in cell volume. In other words, the product $\beta_t \cdot h$ in Eq. 1 would remain largely unchanged, and this would not introduce any additional error into the calculation of P_{HCO3}.

4. pH_i Calibration. Conversion of BCECF fluorescence ratios to pH_i values was based here on calibration data obtained using nigericin (a K^+/H^+ antiporter) and pH calibration solutions with high K^+ concentrations to clamp pH_i to known values. Numerous studies have shown that other calibration methods can yield slightly differing results (e.g., Eisner et al., 1989; Hegyi et al., 2004; Taylor et al., 2006). Consequently, there is the possibility that pH_i may have been systematically over- or underestimated by as much as 0.1 pH units in these experiments, which could also have led to sizeable errors in estimating P_{HCO3}. On the other hand, the fact that the steady-state pH_i values approached at the three different V_a values were close to those predicted for HCO_3^- equilibrium argues against there being a systematic calibration error of this kind.

Contribution of CFTR to Apical HCO_3^- Secretion

Clearly, there is a considerable margin of uncertainty in our estimate of P_{HCO3}. However, it is probably safe to say that P_{HCO3} lies between 0.05 and 0.2 μm s^{-1}. Because this may be the first study to estimate absolute, rather than relative, HCO_3^- permeability in native epithelium, it is difficult to make comparisons with previous work. A P_{HCO3} value of 0.1 μm s^{-1} under the conditions of these experiments would be equivalent to a HCO_3^- conductance of around 2 mS cm^{-2} (assuming a Goldman-Hodgkin-Katz model for channel permeation), which is similar to estimates of apical HCO_3^- conductance in the CFTR-expressing Calu-3 cell line (1.1 mS cm^{-2}; Illek et al., 1999). Others have estimated apical HCO_3^- permeability in bovine corneal endothelium (Bonanno et al., 1999) and guinea pig colon (Endeward and Gros, 2005), but unfortunately without taking into account the effects of membrane potential and/or the contribution of anion exchangers.

To put our estimate of P_{HCO3} into context with regard to ductal secretion in the pancreas, we return to a calculation that we published previously (Ishiguro et al., 2002b). Stimulated interlobular ducts from guinea pig have been shown to secrete HCO_3^- at a rate of ∼0.5 nmol sec^{-1} cm^{-2} (Ishiguro et al., 1998) under conditions similar to those used in the present study. (Because the duct lumen was not perfused in those experiments, we have to bear in mind the possibility that perfusion may influence secretory rate.) We also know the electrochemical gradient for HCO_3^- from measurements of intracellular HCO_3^- concentration (20 mM) and membrane potential (−60 mV). It is therefore possible to calculate the apical HCO_3^- permeability that would be required for all of the secreted HCO_3^- to cross the apical membrane via a conductive pathway. The figure we obtained was 0.25 μm sec^{-1} (Ishiguro et al., 2002b), so our estimate of 0.05–0.2 μm sec^{-1} for P_{HCO3} in the present study is clearly of the right order of magnitude. Given the degree of uncertainty in this value, it would be dangerous to put a precise figure on the fraction of the secreted HCO_3^- that crosses the apical membrane via a conductive pathway. However, there are good reasons for supposing that it is at least one half of the total HCO_3^- flux, and it may be considerably more. Moreover, there is strong evidence to suggest that it is mediated directly by CFTR.

CFTR has not previously been thought to provide a major route for HCO_3^- secretion in the pancreatic duct. This is because estimates of the P_{HCO3}/P_{Cl} ratio (0.2–0.5; Poulsen et al., 1994; Linsdell et al., 1997; Illek et al., 1999; O'Reilly et al., 2000) were considered to be too low, and it was expected that the secretion of Cl^- would greatly exceed that of HCO_3^-. The problem with the alternative hypothesis, namely that HCO_3^- would be secreted predominantly by exchange with luminal Cl^-, was that a neutral $1HCO_3^-$:$1Cl^-$ exchanger would reverse and reabsorb HCO_3^- during maximal secretion when the luminal HCO_3^- concentration is ∼140 mM. The discovery that the apical anion exchanger is SLC26A6 and that it probably operates electrogenically with a $2HCO_3^-$:$1Cl^-$ stoichiometry may prove to be very important. With a

2:1 stoichiometry, the exchanger would be very close to equilibrium when the luminal HCO_3^- concentration reaches 140 mM, but it could nonetheless play a significant role, particularly if the majority of the HCO_3^- is secreted via a conductive pathway (Steward et al., 2005; Ishiguro et al., 2007b). Studies of ductal function in slc26a6-null mice (a species which unfortunately secretes rather little HCO_3^-) have so far yielded conflicting and inconclusive results (Wang et al., 2006; Ishiguro et al., 2007a).

The idea that CFTR provides a significant conductive pathway for HCO_3^- secretion is supported by several observations. It is now known that the anion selectivity of CFTR is regulated by both intracellular and extracellular factors (O'Reilly et al., 2000; Reddy and Quinton, 2003). In particular, low extracellular Cl^- concentrations, as are found in the duct lumen during maximal secretion, have been shown to increase the permeability of CFTR to HCO_3^- relative to Cl^- (Shcheynikov et al., 2004; Wright et al., 2004), although this interpretation has recently been challenged (Tang et al., 2008). This effect, combined with a fall in the driving force for Cl^- secretion (owing to the limited capacity of the basolateral Cl^- uptake pathways; Fernandez-Salazar et al., 2004) would tend to favor HCO_3^- rather than Cl^- efflux via CFTR during maximal secretion. A similar conclusion has been drawn previously both in experimental studies of Calu-3 airway epithelial cells (Devor et al., 1999) and in computational modeling studies of the pancreatic duct (Sohma et al., 2000; Whitcomb and Ermentrout, 2004).

In summary, we have demonstrated voltage-driven fluxes of HCO_3^- across the apical membrane of pancreatic duct cells that are not dependent on the presence of Cl^- or luminal Na^+, are largely blocked by $CFTR_{inh}$-172, and are absent in ducts isolated from ΔF mice. Our estimate of ~0.1 μm sec^{-1} for the apical HCO_3^- permeability of guinea pig duct cells under physiological conditions is close to the value required to account for the observed rate of HCO_3^- secretion. We therefore conclude that a significant fraction of the secreted HCO_3^- enters the ductal lumen via CFTR. It seems likely that the remainder is secreted by a $2HCO_3^-$:$1Cl^-$ exchanger (SLC26A6) operating close to equilibrium.

This study was supported by the Japan Society for the Promotion of Science and the Ministry of Health, Labor, and Welfare, Japan.

Angus C. Nairn served as editor.

Submitted: 22 September 2008
Accepted: 16 January 2009

REFERENCES

Ahmed, N., M. Corey, G. Forstner, J. Zielenski, L.-C. Tsui, L. Ellis, E. Tullis, and P. Durie. 2003. Molecular consequences of cystic fibrosis transmembrane conductance regulator (CFTR) gene mutations in the exocrine pancreas. *Gut.* 52:1159–1164.

Argent, B.E., S. Arkle, M.J. Cullen, and R. Green. 1986. Morphological, biochemical and secretory studies on rat pancreatic ducts maintained in tissue culture. *Q. J. Exp. Physiol.* 71:633–648.

Argent, B.E., M.A. Gray, M.C. Steward, and R.M. Case. 2006. Cell physiology of pancreatic ducts. *In* Physiology of the Gastrointestinal Tract, fourth edition. L.R. Johnson, K.E. Barrett, F.K. Ghishan, J.L. Merchant, H.M. Said, and J.D. Wood, editors. Elsevier Academic Press, New York. 1371–1396.

Arkle, S., C.M. Lee, M.J. Cullen, and B.E. Argent. 1986. Isolation of ducts from the pancreas of copper-deficient rats. *Q. J. Exp. Physiol.* 71:249–265.

Bonanno, J.A., Y. Guan, S. Jelamskii, and X.J. Kang. 1999. Apical and basolateral CO_2-HCO_3^- permeability in cultured bovine corneal endothelial cells. *Am. J. Physiol.* 277:C545–C553.

Chernova, M.N., L. Jiang, D.J. Friedman, R.B. Darman, H. Lohi, J. Kere, D.H. Vandorpe, and S.L. Alper. 2005. Functional comparison of mouse slc26a6 anion exchanger with human SLC26A6 polypeptide variants: differences in anion selectivity, regulation, and electrogenicity. *J. Biol. Chem.* 280:8564–8580.

Cohn, J.A. 2005. Reduced CFTR function and the pathobiology of idiopathic pancreatitis. *J. Clin. Gastroenterol.* 39:s70–s77.

Crawford, I., P.C. Maloney, P.L. Zeitlin, W.B. Guggino, S.C. Hyde, H. Turley, K.C. Gatter, A. Harris, and C.F. Higgins. 1991. Immunocytochemical localization of the cystic fibrosis gene product CFTR. *Proc. Natl. Acad. Sci. USA.* 88:9262–9266.

Devor, D.C., A.K. Singh, L.C. Lambert, A. DeLuca, R.A. Frizzell, and R.J. Bridges. 1999. Bicarbonate and chloride secretion in Calu-3 human airway epithelial cells. *J. Gen. Physiol.* 113:743–760.

Edsall, J.T., and J. Wyman. 1958. Biophysical Chemistry. Vol. 1. Academic Press, New York. 555–561.

Egerbacher, M., and P. Bock. 1997. Morphology of the pancreatic duct system in mammals. *Microsc. Res. Tech.* 37:407–417.

Eisner, D.A., N.A. Kenning, S.C. O'Neill, G. Pocock, C.D. Richards, and M. Valdeolmillos. 1989. A novel method for absolute calibration of intracellular pH indicators. *Pflugers Arch.* 413:553–558.

Endeward, V., and G. Gros. 2005. Low carbon dioxide permeability of the apical epithelial membrane of guinea-pig colon. *J. Physiol.* 567:253–265.

Fernandez-Salazar, M.P., P. Pascua, J.J. Calvo, M.A. Lopez, R.M. Case, M.C. Steward, and J.I. San Roman. 2004. Basolateral anion transport mechanisms underlying fluid secretion by mouse, rat and guinea-pig pancreatic ducts. *J. Physiol.* 556:415–428.

Foskett, J.K. 1990. $[Ca^{2+}]_i$ modulation of Cl^- content controls cell volume in single salivary acinar cells during fluid secretion. *Am. J. Physiol.* 259:C998–C1004.

Fujiki, K., H. Ishiguro, S.B. Ko, N. Mizuno, Y. Suzuki, T. Takemura, A. Yamamoto, T. Yoshikawa, M. Kitagawa, T. Hayakawa, et al. 2004. Genetic evidence for CFTR dysfunction in Japanese: background for chronic pancreatitis. *J. Med. Genet.* 41:e55.

Hegyi, P., Z. Rakonczay, M.A. Gray, and B.E. Argent. 2004. Measurement of intracellular pH in pancreatic duct cells: a new method for calibrating the fluorescence data. *Pancreas.* 28:427–434.

Illek, B., A.W.K. Tam, H. Fischer, and T.E. Machen. 1999. Anion selectivity of apical membrane conductance of Calu 3 human airway epithelium. *Pflugers Arch.* 437:812–822.

Ishiguro, H., M.C. Steward, A.R.G. Lindsay, and R.M. Case. 1996. Accumulation of intracellular HCO_3^- by Na^+-HCO_3^- cotransport in interlobular ducts from guinea-pig pancreas. *J. Physiol.* 495:169–178.

Ishiguro, H., S. Naruse, M.C. Steward, M. Kitagawa, S.B.H. Ko, T. Hayakawa, and S. Naruse. 1998. Fluid secretion in interlobular ducts isolated from guinea-pig pancreas. *J. Physiol.* 511:407–422.

Ishiguro, H., S. Naruse, M. Kitagawa, A. Suzuki, A. Yamamoto, T. Hayakawa, R.M. Case, and M.C. Steward. 2000. CO_2 permeability

and bicarbonate transport in microperfused interlobular ducts isolated from guinea-pig pancreas. *J. Physiol.* 528:305–315.

Ishiguro, H., S. Naruse, M. Kitagawa, T. Mabuchi, T. Kondo, T. Hayakawa, R.M. Case, and M.C. Steward. 2002a. Chloride transport in microperfused interlobular ducts isolated from guinea-pig pancreas. *J. Physiol.* 539:175–189.

Ishiguro, H., M.C. Steward, Y. Sohma, T. Kubota, M. Kitagawa, T. Kondo, R.M. Case, T. Hayakawa, and S. Naruse. 2002b. Membrane potential and bicarbonate secretion in isolated interlobular ducts from guinea-pig pancreas. *J. Gen. Physiol.* 120:617–628.

Ishiguro, H., W. Namkung, A. Yamamoto, Z. Wang, R.T. Worrell, J. Xu, M.G. Lee, and M. Soleimani. 2007a. Effect of Slc26a6 deletion on apical Cl^-/HCO_3^- exchanger activity and cAMP-stimulated bicarbonate secretion in pancreatic duct. *Am. J. Physiol.* 292:G447–G455.

Ishiguro, H., M. Steward, and S. Naruse. 2007b. Cystic fibrosis transmembrane conductance regulator and SLC26 transporters in HCO_3^- secretion by pancreatic duct cells. *Acta Physiologica Sinica.* 59:465–476.

Ko, S.B., N. Shcheynikov, J.Y. Choi, X. Luo, K. Ishibashi, P.J. Thomas, J.Y. Kim, K.H. Kim, M.G. Lee, S. Naruse, and S. Muallem. 2002. A molecular mechanism for aberrant CFTR-dependent HCO_3^- transport in cystic fibrosis. *EMBO J.* 21:5662–5672.

Linsdell, P., J.A. Tabcharani, J.M. Rommens, Y.X. Hou, X.B. Chang, L.C. Tsui, J.R. Riordan, and J.W. Hanrahan. 1997. Permeability of wild-type and mutant cystic fibrosis transmembrane conductance regulator chloride channels to polyatomic anions. *J. Gen. Physiol.* 110:355–364.

Lohi, H., M. Kujala, E. Kerkela, U. Saarialho-Kere, M. Kestila, and J. Kere. 2000. Mapping of five new putative anion transporter genes in human and characterization of SLC26A6, a candidate gene for pancreatic anion exchanger. *Genomics.* 70:102–112.

Marino, C.R., L.M. Matovcik, F.S. Gorelick, and J.A. Cohn. 1991. Localization of the cystic fibrosis transmembrane conductance regulator in pancreas. *J. Clin. Invest.* 88:712–716.

Novak, I., and R. Greger. 1988. Electrophysiological studies of transport systems in isolated perfused pancreatic ducts: properties of the basolateral membrane. *Pflugers Arch.* 411:546–553.

Novak, I., and R. Greger. 1991. Effect of bicarbonate on potassium conductance of isolated perfused rat pancreatic ducts. *Pflugers Arch.* 411:546–553.

O'Reilly, C.M., J.P. Winpenny, B.E. Argent, and M.A. Gray. 2000. Cystic fibrosis transmembrane conductance regulator currents in guinea pig pancreatic duct cells: inhibition by bicarbonate ions. *Gastroenterology.* 118:1187–1196.

Poulsen, J.H., H. Fischer, B. Illek, and T.E. Machen. 1994. Bicarbonate conductance and pH regulatory capability of cystic fibrosis transmembrane conductance regulator. *Proc. Natl. Acad. Sci. USA.* 91:5340–5344.

Reddy, M.M., and P.M. Quinton. 2003. Control of dynamic CFTR selectivity by glutamate and ATP in epithelial cells. *Nature.* 423:756–760.

Shcheynikov, N., K.H. Kim, K.M. Kim, M.R. Dorwart, S.B. Ko, H. Goto, S. Naruse, P.J. Thomas, and S. Muallem. 2004. Dynamic control of cystic fibrosis transmembrane conductance regulator Cl^-/HCO_3^- selectivity by external Cl^-. *J. Biol. Chem.* 279:21857–21865.

Shcheynikov, N., Y. Wang, M. Park, S.B. Ko, M. Dorwart, S. Naruse, P.J. Thomas, and S. Muallem. 2006. Coupling modes and stoichiometry of Cl^-/HCO_3^- exchange by slc26a3 and slc26a6. *J. Gen. Physiol.* 127:511–524.

Sohma, Y., M.A. Gray, Y. Imai, and B.E. Argent. 2000. HCO_3^- transport in a mathematical model of the pancreatic ductal epithelium. *J. Membr. Biol.* 176:77–100.

Steward, M.C., H. Ishiguro, and R.M. Case. 2005. Mechanisms of bicarbonate secretion in the pancreatic duct. *Annu. Rev. Physiol.* 67:377–409.

Szalmay, G., G. Varga, F. Kajiyama, X.-S. Yang, T.F. Lang, R.M. Case, and M.C. Steward. 2001. Bicarbonate and fluid secretion evoked by cholecystokinin, bombesin and acetylcholine in isolated guinea-pig pancreatic ducts. *J. Physiol.* 535:795–807.

Tang, L., F. Mohammad, and P. Linsdell. 2008. Mechanism of direct bicarbonate transport by the CFTR anion channel. *J. Cyst. Fibros.* In press.

Taylor, C.J., P.A. Nicola, S. Wang, M.A. Barrand, and S.B. Hladky. 2006. Transporters involved in regulation of intracellular pH in primary cultured rat brain endothelial cells. *J. Physiol.* 576:769–785.

Wang, Y.X., A.A. Soyombo, N. Shcheynikov, W.Z. Zeng, M. Dorwart, C.R. Marino, P.J. Thomas, and S. Muallem. 2006. Slc26a6 regulates CFTR activity in vivo to determine pancreatic duct HCO_3^- secretion: relevance to cystic fibrosis. *EMBO J.* 25:5049–5057.

Whitcomb, D.C., and G.B. Ermentrout. 2004. A mathematical model of the pancreatic duct cell generating high bicarbonate concentrations in pancreatic juice. *Pancreas.* 29:e30–e40.

Wright, A.M., X.D. Gong, B. Verdon, P. Linsdell, A. Mehta, J.R. Riordan, B.E. Argent, and M.A. Gray. 2004. Novel regulation of cystic fibrosis transmembrane conductance regulator (CFTR) channel gating by external chloride. *J. Biol. Chem.* 279:41658–41663.

Zeiher, B.G., E. Eichwald, J. Zabner, J.J. Smith, A.P. Puga, P.B. McCray Jr., M.R. Capecchi, M.J. Welsh, and K.R. Thomas. 1995. A mouse model for the delta F508 allele of cystic fibrosis. *J. Clin. Invest.* 96:2051–2064.

Zeng, W., M.G. Lee, M. Yan, J. Diaz, I. Benjamin, C.R. Marino, R. Kopito, S. Freedman, C. Cotton, S. Muallem, and P.J. Thomas. 1997. Immuno and functional characterization of CFTR in submandibular and pancreatic acinar and duct cells. *Am. J. Physiol.* 273:C442–C455.